PART V

OPTICAL MEASUREMENTS AND NAVIGATION PHENOMENA

by

D. Alexander Koso

D. ALEXANDER KOSO

Assistant Director, Instrumentation Laboratory
Massachusetts Institute of Technology

D. Alexander Koso, Assistant Director of Instrumentation Laboratory, Massachusetts Institute of Technology, heads the Laboratory group responsible for development of the optical subsystem — space sextant, scanning telescope and the associated electronics — used in the guidance system the Laboratory is developing for the Project Apollo spacecraft.

Mr. Koso was born in Bratislava, Czechoslovakia, March 13, 1935, and came to the United States in 1949. He was graduated from University High School, Minneapolis, Minn., in 1952. He received both the B.S. and M.S. degrees from M.I.T. in electrical engineering in 1957 and the degree of Electrical Engineer from M.I.T. in 1959.

While an undergraduate at M.I.T., Mr. Koso studied under the Institute's cooperative plan and was employed by the Philco Corporation. As a graduate student studying for the E.E. degree, he was a research assistant at the M.I.T. Electronic Systems Laboratory.

Mr. Koso joined the Instrumentation Laboratory in 1959 and worked a few years on navigation studies for manned boost-glide space vehicles. He was appointed an Assistant Director in 1963.

Part V

OPTICAL MEASUREMENTS AND NAVIGATION PHENOMENA

INTRODUCTION

During the orbital and midcourse phases of a space mission, inertial components (due to a lack of force) can no longer provide information about the position of the vehicle. The gyroscope can be used to provide an artificial set of fixed stars usable as a basic reference for measurements. However, external sensors have to be used to update the position information within the vehicle.

During the orbital phases of a mission, it is possible to treat the navigational problem with relative ease because one can write a set of linear constant coefficient equations which describe the propagation of errors with time. Each measurement then provides a linear equation between certain of these errors. In this chapter on-board measurements are considered which can be used to determine the orbit of a satellite.

CHAPTER V-1

NAVIGATION IN ORBIT

ERROR PROPAGATION IN ORBIT

The equations of motion in this analysis are written in polar coordinates to make linear approximation of these equations easier. Thus, the equations presented are closer to the equations of a local-vertical system; however, the analysis applies irrespective of the coordinate system used in the actual computation.

The equations of motion in polar coordinates are:

$$\ddot{R} = F_R + R\Omega^2 - E/R^2 \qquad \text{(V-1a)}$$

$$R\frac{d^2\theta}{dt^2} = R\dot{\Omega} = F_\theta - 2R\Omega \qquad \text{(V-1b)}$$

where F_R and F_θ are the forces (per unit mass of the vehicle) in the radial and range direction respectively as illustrated in Fig. V-1.

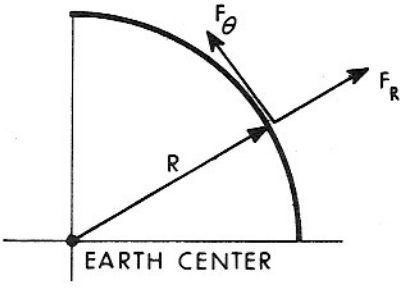

Figure V-1

For the purpose of analysis, set:

$$R = r_o + r \tag{V-2a}$$

$$\Omega = \omega_o + \omega \tag{V-2b}$$

where r_o and ω_o are constants.
Thus,

$$\dot{R} = \dot{r};\ \ddot{R} = \ddot{r};\ \dot{\Omega} = \dot{\omega};\ \theta - \omega_o t = \int_o^t \omega(x)dx$$

One can also assume without loss of generality that:

$$\omega_o = E/r_o^3 \tag{V-3}$$

If r_o is assumed to be about 300 kilometers above mean earth radius, then for orbits ranging from 150 to 450 km altitude:

$$r/r_o < .02 \tag{V-4}$$

Similarly:

$$\omega/\omega_o < .05 \tag{V-5}$$

Thus, the equations of motion can be linearized for satellites confined to nearly circular orbits.

Under the assumption that:

$$E/R^2 = E/r_o^2 - [2E/r_o^3]r \tag{V-6}$$

Equations V-1a and V-1b can be written as:

$$\ddot{r} = F_R + (r_o + r)(\omega_o^2 + 2\omega_o\omega + \omega^2) - E/r_o^2 + 2E/r_o^3\, r \tag{V-7a}$$

$$(r_o + r)\dot{\omega} = F_\theta - 2\dot{r}(\omega_o + \omega) \qquad \text{(V-7b)}$$

Substitution of Eq. V-3 into V-7a and V-7b gives:

$$\ddot{r} = F_R + 3\omega_o^2 r + 2\omega_o\omega(r_o + r) + (r_o + r)\omega^2 \qquad \text{(V-8a)}$$

$$(r_o + r)\dot{\omega} = F_\theta - 2(\omega_o + \omega)r \qquad \text{(V-8b)}$$

Using the approximations of Eqs. V-4 and V-5,

$$r << r_o;\ \omega << \omega_o$$

Eqs. V-8a and V-8b become:

$$\ddot{r} = F_R + 3\omega_o^2 r + 2\omega_o r_o \omega \qquad \text{(V-9a)}$$

$$r_o\dot{\omega} = F_\theta - 2\omega_o\dot{r} \qquad \text{(V-9b)}$$

Equations V-9a and V-9b represent very closely the errors in the position computation of an orbiting vehicle. For relatively short flights, the two force inputs F_R and F_θ are also negligible, so that the major contribution of error is due to the uncertainty in initial conditions at the end of injection into orbit.

There is another error which can exist in an orbit determination. This one is due to a lack of knowledge of the exact direction of the ω_o vector (see Fig. V-2).

If the angular displacement is small, the error in the out of plane position is given by:

$$\Phi = E_\Phi \cos(\omega_o + \omega)t + \frac{\dot{E_\Phi}}{\omega_o} \sin(\omega_o + \omega)t \qquad \text{(V-10)}$$

For relatively small range errors, the ω term can be neglected. From a control viewpoint, the error in the position computation can be represented very closely by the two linear constant-coefficient systems shown in Fig. V-3. One set of equations is fourth order, the other second order. E_* is the particular initial condition error.

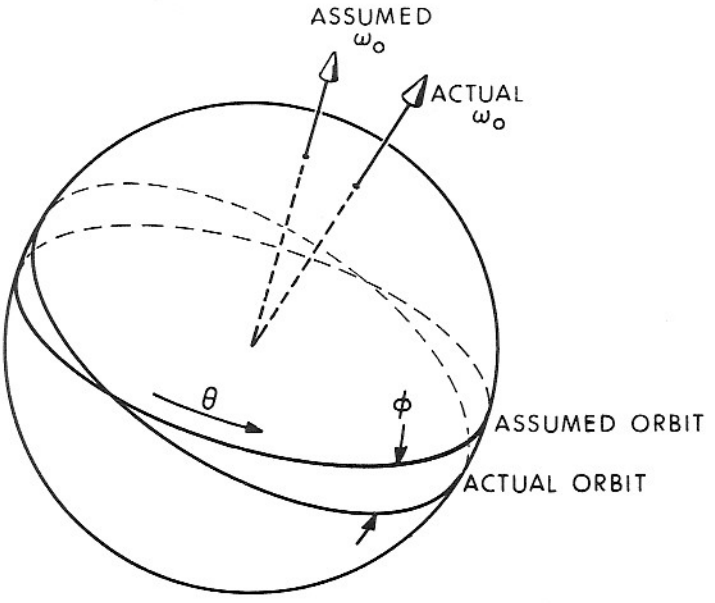

Fig. V-2 Orbital Geometry

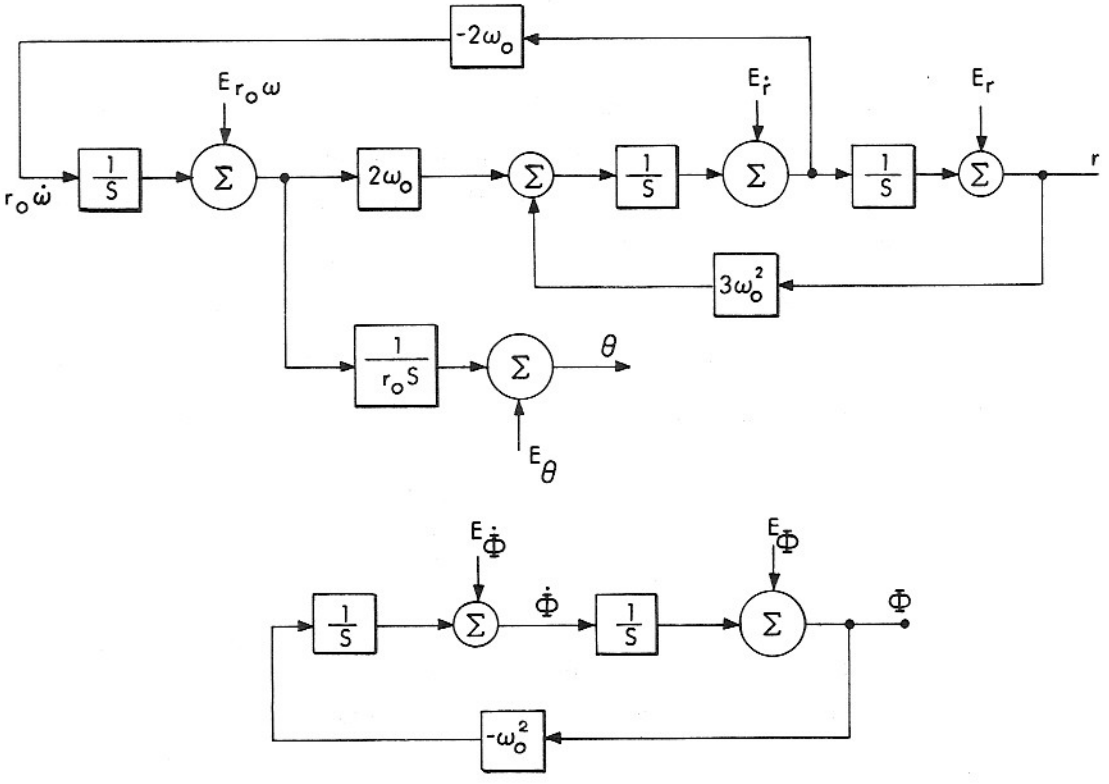

Fig. V-3 Block Diagram of Error Propagation

Table V-1 Summary of Errors due to Initial Conditions at Some Time, τ, after Insertion into Orbit

Error Source	Range	Range Rate	Altitude	Altitude Rage	Track	Track Rate
E_r	$\frac{6}{r_o}(\sin \omega_o t - \omega_o t)$	$6\omega_o(\cos \omega_o t - 1)$	$3(1 - \cos \omega_o t) + 1$	$3\omega_o \sin \omega_o t$	0	0
$E_{\dot{r}}$	$\frac{2}{r_o \omega_o}(\cos \omega_o t - 1)$	$-2 \sin \omega_o t$	$\frac{1}{\omega_o} \sin \omega_o t$	$\cos \omega_o t$	0	0
E_θ	1	0	0	0	0	0
$E_{r_{\theta\omega}}$	$\frac{4}{r_o \omega_o}(\sin \omega_o t - \omega_o t) + \frac{1}{r_o} t$	$4(\cos \omega_o t - 1) + 1$	$\frac{2}{\omega_o}(1 - \cos \omega_o t)$	$2 \sin \omega_o t$	0	0
E_ϕ	0	0	0	0	$\cos \omega_o t$	$\frac{1}{\omega_o} \sin \omega_o t$
$E_{\dot{\phi}}$	0	0	0	0	$\omega_o \sin \omega_o t$	$\cos \omega_o t$

Two conclusions can be drawn from this Table:

Only range error grows with time

There is no error coupling between range and track errors

Generally, depending on the particular problem on hand, the navigational system has to be able to determine the position and velocity errors at some time, T, after injection into orbit. However, since this time, T, depends on a specific mission phase, only the problem of initial condition determination will be treated here. The actual errors at the specified time, T, can then easily be obtained from the initial condition errors and the expressions of Table V-1.

POSSIBLE MEASUREMENTS

As can be seen from the block diagram, Fig. V-3, there are six possible sources of error which have to be considered. The measurements which are taken have to provide some information about the Φ and θ errors. Thus, while a good altimeter can be used to determine $E_{r_{\omega}^{o}}$, $E_{\dot{r}}$ and E_{r}, it cannot provide information about E_{θ}, $E_{\dot{\Phi}}$, and $E_{\dot{\Phi}}$. Similarly, a velocity meter, even if it could provide information about $E_{\dot{\Phi}}$ and $E_{\dot{\Phi}}$ in addition to the variables provided for by the altimeter, would provide no information about E_{θ}.

While most of these considerations are of academic interest on the earth where radar tracking coverage is provided, they do become important during lunar operations, where - especially on the back side of the moon - ground based information is not available. Thus, the following measurements have been considered:

1. Bearing measurements to known landmarks
2. Bearing measurements to unknown landmarks
3. Star occultation measurements
4. Star horizon measurements
5. Star known landmark measurements

Measurements of two or three horizons simultaneously were rejected because the lines of sight have to be able to see almost a full hemisphere. This requires a sensor too close to the skin of the vehicle to make this type of a measurement feasible.

In midcourse, where the subtended angle of the planet is smaller, and this measurement becomes feasible from an equipment standpoint, the error sensitivities are so low that the accuracy requirement was deemed not feasible.

While this is not an exhaustive list of possible measurements, it does cover a large variety of applications and it can be instrumented with a relatively simple optical system.

KNOWN LANDMARK BEARING MEASUREMENT

Consider a known point on the earth' s surface and an assumed vehicle position as shown in Fig. V-4. The assumed position of the vehicle at time, T, is at a range θ_o (T) and ϕ_o (T) and an altitude H_o(T) from the known landmark. Now consider a projection of the landmark into the assumed orbital plane as shown in Fig. V-5. The angle α is the angle between the local horizontal at the landmark, and the projection of the vehicle into the assumed orbital plane.

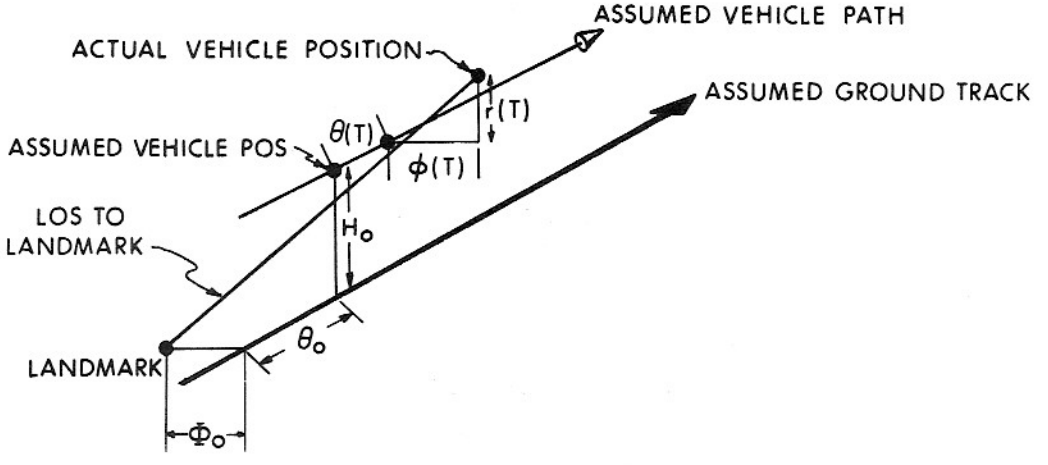

Fig. V-4 Known Landmark Measurement Geometry

Figure V-5 provides the first equation of orbit determination from a bearing measurement to a known landmark:

$$\frac{\theta_o(T) + \theta(T)}{H_o(T) + r(T)} = \cot \alpha \qquad \text{(V-11)}$$

Now consider a projection of Fig. V-4 into a plane which is orthogonal to the assumed orbital plane and which also contains the landmark local vertical as shown in Fig. V-6.

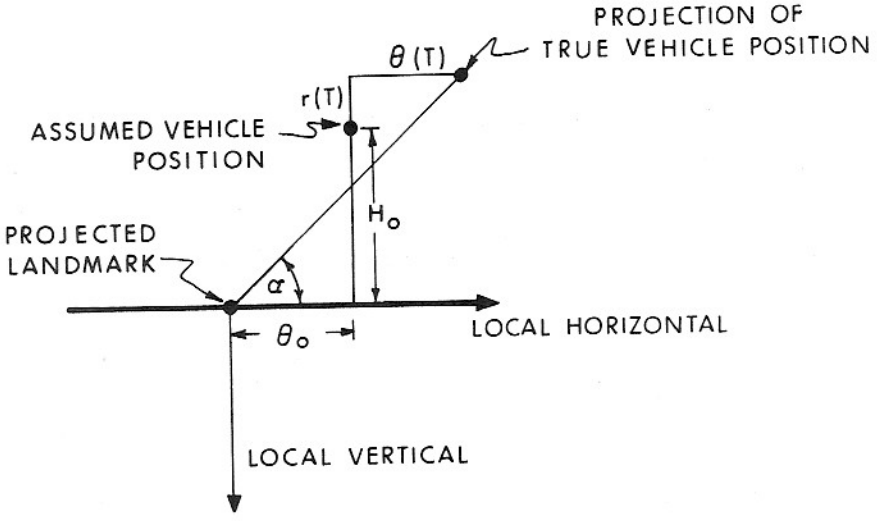

Fig. V-5 In Plane Measurement Geometry

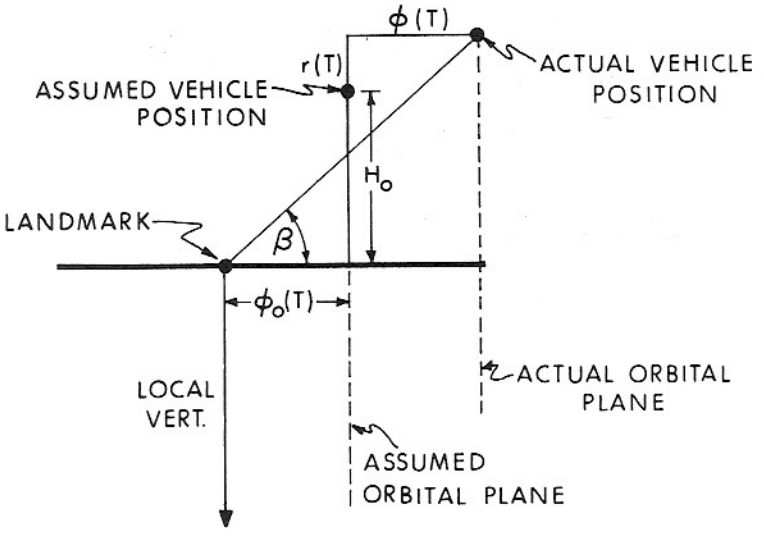

Fig. V-6 Out of Plane Measurement Geometry

This measurement provides the second equation of orbit determination:

$$\frac{\Phi_o(T) + \Phi(T)}{H_o(T) + r(T)} = \cot \beta \qquad \text{(V-12)}$$

The cotangent has been chosen because $H_o(T) + r(T) > 0$ at all times and the equations are well behaved.

Let us assume that a landmark can be tracked when the angle between the local vertical at the landmark and the line of sight is less than 45^o. For a 150 kilometer orbit, this means that the landmark can be tracked for a period of less than 40 seconds. The exact amount depends on the distance between the landmark and the ground track of the vehicle.

Consider the time, T, when the landmark is first acquired. It is immediately possible to write two equations, V-11 and V-12, in the three unknowns $r(T_1)$, $\theta(T_1)$, and $\phi(T_1)$. Consider now the determination of other variables at time, T_1, by further bearing measurements to the same landmark. At the time, $t > T_1$, the position errors of the vehicle will have changed. The new variables are:

$$\theta(t) = \theta(T_1) + \omega(T_1)(t-T_1) \qquad \text{(V-13a)}$$

$$r(t) = r(T_1) + \dot{r}(T_1)(t-T_1) + r_o\omega_o\theta(T_1) \qquad \text{(V-13b)}$$

$$\phi(t) = \phi(T_1) + \dot{\phi}(T_1)(t-T_1) \qquad \text{(V-13c)}$$

Substituting Eqs. V-13 into V-11 and V-12 provides a complete solution to the orbital navigational problem:

$$\theta(T_1)+(t-T_1)\omega(T_1)-\cot\alpha(t)r(T_1)-\cot\alpha(t)(t-T_1)[\dot{r}(T_1)+ r_o\omega_o\theta(T_1)] = \cot\alpha(T)H_o(t)-\theta_o(t) \qquad \text{(V-14a)}$$

$$\phi(T_1)+(t-T_1)\dot{\phi}(T_1)-\cot\alpha(t)r(T_1)-\cot\alpha(t)(t-T_1)[\dot{r}(T_1)+r_o\omega_o\theta(T_1)] = \cot\alpha(T)H_o(t)-\phi_o(t) \qquad \text{(V-14b)}$$

However, four bearing measurements to a single landmark are required before Eqs. V-14a and V-14b can be solved. Three measurements do provide six equations in the six unknowns; but they are not independent.

UNKNOWN LANDMARK BEARING MEASUREMENT

When the point on the earth' s surface has unknown coordinates, the navigational system has to rely on the changes in the tracking angle as the vehicle passes over the landmark.

Let us assume that the astronaut can lock-on to an identifiable but otherwise unkncwn point on the earth' s surface when the angle between the computed (or assumed) velocity vector and the line of sight to the point is approximately 45°. The exact number will depend on the skill of the astronaut and on the range error which the navigational system has accumulated by the time of the measurement.

Consider the measurement geometry of Fig. V-7 and the projections of this geometry into the orbital plane as shown in Fig. V-8.

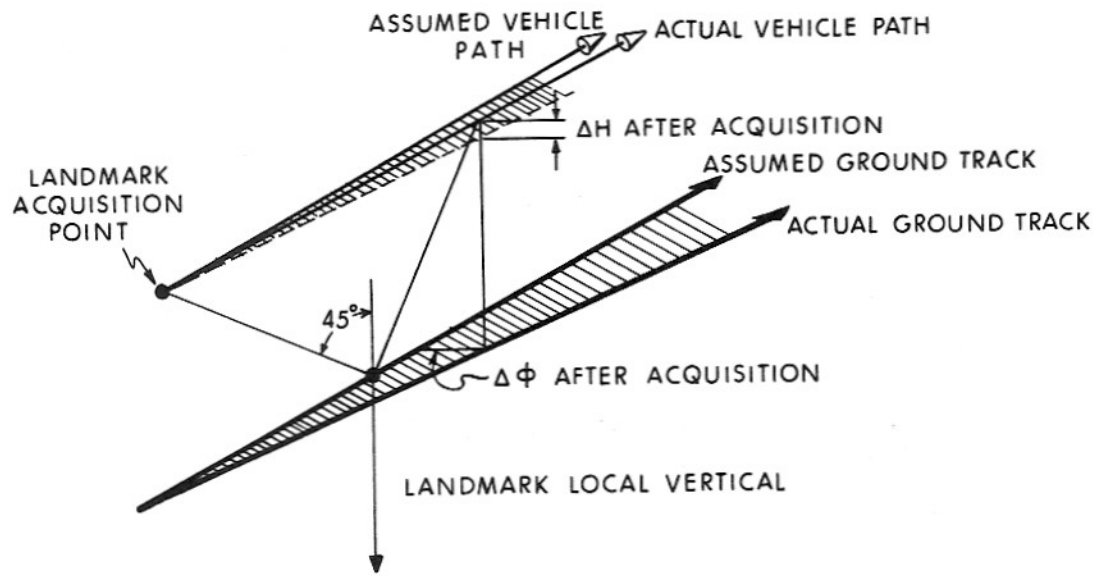

Figure V-7

Measured Geometry for an Unknown Landmark

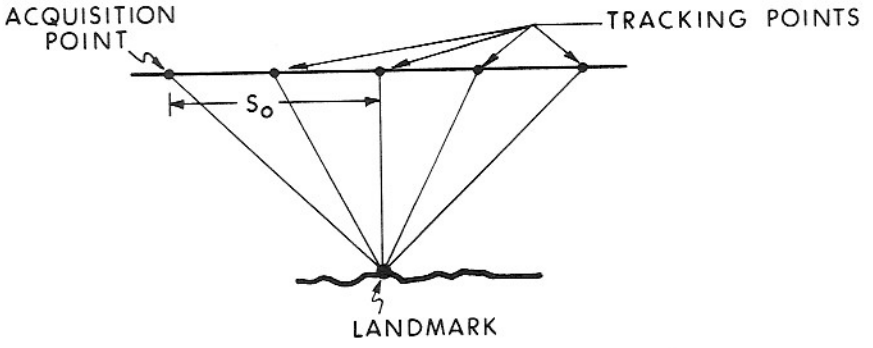

Fig. V-8 Nominal Tracking Sequence

The problem is the determination of the errors: $r(T_1)$, $\dot{r}(T_1)$, $\theta(T_1)$, $r_o\omega(T_1)$, $\phi(T_1)$, $\dot{\phi}(T_1)$ at the time of unknown landmark acquisition. As will be seen, it is not possible to determine all of the errors after the tracking of a single landmark; at least four landmarks have to be tracked before all of the orbital parameters of a vehicle can be determined.

Let us assume that the distance between the intersection of the landmark local vertical and assumed velocity vector and the point where tracking begins is S_o (Fig. V-8). For a general time, τ, after T_1 (T_1 is the time when tracking begins), the computed bearing measurement is given by:

$$\cot \alpha_c = \frac{S_o - r_o \omega_o \tau}{H_o} \qquad \text{(V-15)}$$

This variation in the bearing angle has to be compared to the angle which actually gets measured.

Consider first an erroneous altitude of the vehicle $r(T_1)$.

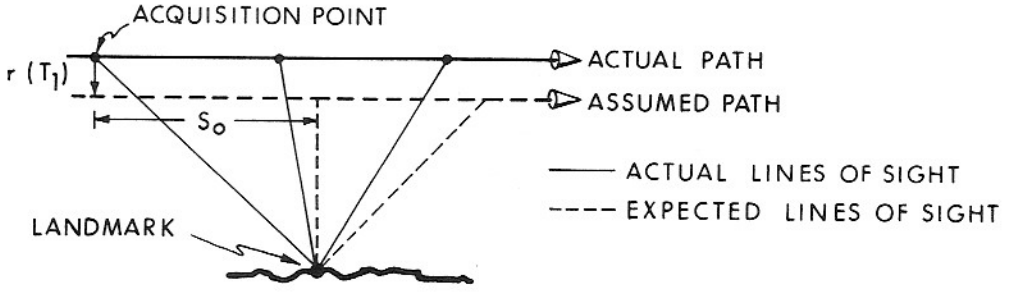

Fig. V-9 Tracking with an Erroneous Vehicle or Landmark Altitude

As can be seen from Fig. V-9, it is impossible to determine the difference between an altitude error in the vehicle path and a lack of knowledge in the altitude of the landmark. For a general time, τ, after T_1, the actual bearing measurement give

$$\cot \alpha_a = \frac{S_o - r_o \omega_o \tau}{H_o + r(T_1) - \Delta H} + \frac{\cot \alpha(0)(r(T_1) - \Delta H)}{H_o + r(T_1) - \Delta H} \qquad \text{(V-}$$

where ΔH is the altitude uncertainty of the landmark.

If the vehicle has an error $\omega(T_1)$ when tracking begins, then the measurement geometry is as shown in Fig. V-10.

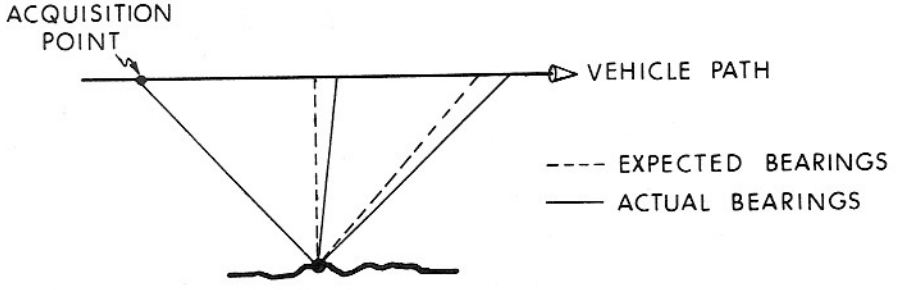

Fig. V-10 Tracking with an Erroneous Velocity Along Range

The actual bearing measurements in this case are:

$$\cot \alpha_a = \frac{S_o - (\omega_o + \omega(T_1)) r_o \tau}{H_o} \qquad \text{(V-}$$

Again τ is the time after landmark acquisition.

Tracking with an initial vertical velocity error provides the geometry of Fig. V-11. In this case the bearing measurements are:

$$\cot \alpha_a = \frac{S_o - r_o \omega_o \tau}{H_o + \dot{r}(T_1)\tau} \qquad \text{(V-}$$

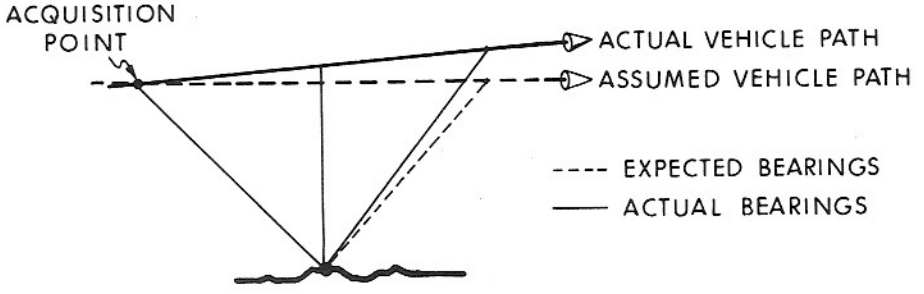

Fig. V-11 Tracking with an Erroneous Vertical Velocity

An initial range ($\theta(T_1)$) error appears identical to a vertical velocity error because at the time, T_1, the computed and actual velocity vectors differ by the angle $\theta(T_1)$ as shown in Fig. V-12. Thus again it is impossible to distinguish between a range error at time, T_1, and a vertical velocity error at time, T_1.

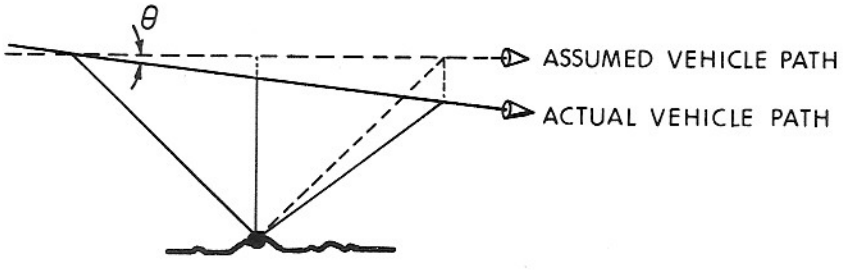

Figure V-12 Tracking with an Erroneous Range Error

The bearing measurement made along the actual trajectory is:

$$\cot \alpha_a = \frac{S_o - r_o \omega_o \tau}{H_o - \theta(T_1) r_o \omega_o \tau} \qquad \text{(V-19)}$$

Since the error terms in Eqs. V-16 to V-19 are generally small, further linear approximations of these equations can be made. Using the approximation,

$$\frac{1}{1+\delta} = 1 - \delta$$

Equation V-16 can be approximated by:

$$\cot \alpha_a = \frac{S_o - r_o \omega_o \tau}{H_o} + \frac{r_o \omega (r(T_1) - \Delta H)}{H_o^2} \qquad \text{(V-20)}$$

(since $S_o = H_o \cot \alpha(0)$)

Equation V-17 can be approximated by:

$$\cot \alpha_a = \frac{S_o - r_o \omega_o \tau}{H_o} - \frac{\omega(T_1) r_o}{H_o} \tau \qquad \text{(V-21)}$$

Equation V-18 can be approximated by:

$$\cot \alpha_a = \frac{S_o r_o \omega_o \tau}{H_o} - \frac{S_o \dot{r}(T_1)}{H_o^2} \tau + \frac{r_o \omega_o \dot{r}(T_1)}{H_o^2} \tau^2 \qquad \text{(V-22)}$$

Equation V-19 can be approximated by:

$$\cot \alpha_a = \frac{S_o - r_o \omega_o \tau}{H_o} + \frac{S_o r_o \omega_o \theta(T_1)}{H_o^2} \tau - \frac{r_o^2 \omega_o^2 \theta(T_1)}{H_o^2} \tau^2 \qquad \text{(V-23)}$$

The first term on the right hand side of Eqs. V-20 through V-23 is $\cot \alpha_c$. Thus, one can write in general:

$$\cot \alpha_a - \cot \alpha_c = \frac{1}{H_o^2}\left(r_o\omega_o(r(T_1)-\Delta H)-\frac{r_o}{H_o}\omega(T_1)-S_o(\dot{r}(T_1)-r_o\omega_o\theta(T_1))\right)\tau \quad \text{(V-24)}$$

$$+\frac{r_o\omega_o}{H_o^2}(r(T_1)-r_o\omega_o\theta(T_1))\tau^2$$

When one considers the magnitude of the terms in Eq. V-24, it becomes apparent that the $r_o\omega(T_1)/H_o$ term can also be neglected. This leaves the relatively simple expression:

$$\cot \alpha_a - \cot \alpha_c = \frac{1}{H_o^2}\left(r_o\omega_o(r(T_1)-\Delta H)+S_o(r_o\omega_o\theta(T_1)-\dot{r}(T_1))\right)\tau$$

$$+\frac{r_o\omega_o}{H_o^2}(\dot{r}(T_1)-r_o\omega_o\theta(T_1))\tau^2 \quad \text{(V-25)}$$

To determine the track errors in the vehicle trajectory, consider the projection of Fig. V-7 into a plane normal to the assumed velocity vector. The unknown landmark should also be contained in this plane. This measurement provides no information about the position error ϕ as shown in Fig. V-13.

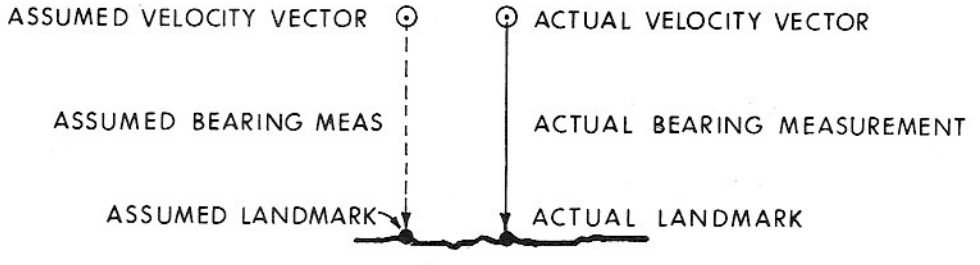

Fig. V-13 Tracking with Erroneous Track Position

However, the measurement does provide information about the track velocity error as shown in Fig. V-14.

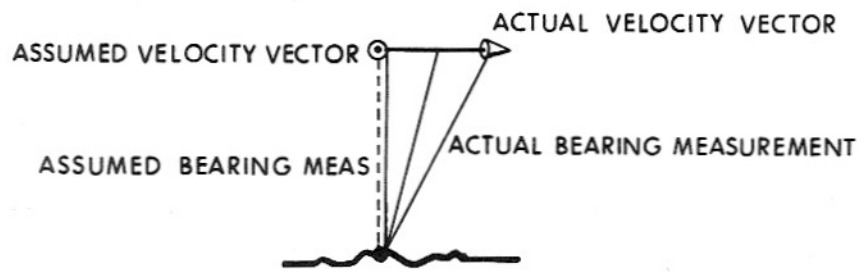

Fig. V-14 Tracking with Erroneous Track Velocity

To determine ϕ, two variables from the in plane component of this measurement hav to be known:

The distance between the landmark and the vehicle velocity vector (just the sum - not the individual components)

The sum of the vertical velocity and range error (again only the sum).

These variables, though, are available from the in plane computation (Eq. V-25). The measurement geometry is as shown in Fig. V-15

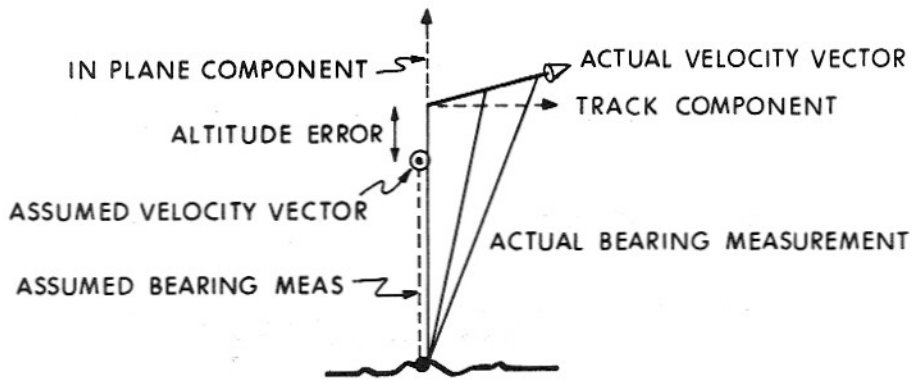

Fig. V-15 Tracking with Erroneous Track Velocity Altitude, Error, and Vertical Velocity Error

Consider the angle, ß, between the assumed bearing measurement and the actual bearing measurement.

$$\sin ß = \frac{\phi r_o \tau}{H_o + r(T_1) - \Delta H + (\dot{r}(T_1) - r_o \omega_o \theta(T_1))\tau} \qquad \text{(V-26)}$$

Depending on the particular orbit, the denominator terms with exception of H_o or possibly $H_o + r(T_1) - \Delta H$ will be negligible. For small values of ß sin ß ≈ ß and in general:

$$\phi = \frac{ß(\tau)(H_o + r(T_1) - \Delta H)}{r_o \tau} \qquad \text{(V-27)}$$

Equations V-25 and V-27 form the two basic equations which have to be solved to determine the orbital parameters when unknown landmarks are used.

Thus, as contrasted with the known landmark measurement, the unknown landmark measurement provides information about the velocity vector of the vehicle. Since each measurement to an unknown landmark provides only one equation for the determination of the four in plane orbital parameter unknowns, it is necessary to track four unknown landmarks to determine the initial condition errors. The first two of these measurements completely determine the track errors. The remaining two track computations - if carried out - serve only for redundancy.

The requirement for four landmarks instead of three appears here again, similarly to the requirements for four bearing measurements to a known landmark.

NAVIGATION USING STAR HORIZON MEASUREMENTS

Let us assume for the moment that it is possible to define an earth horizon by some means. A possible method is discussed in a later section of this paper, where a horizon is defined at approximately 30 KM above the earth's surface. The astronaut then maneuvers the vehicle so that the plane formed by the two lines of sight (star line of sight and horizon line of sight) also contains the center of the earth and measures the angle between the star and horizon.

This places the vehicle on a surface which touches the earth at the earth's

artificial horizon as shown in Fig. V-16.

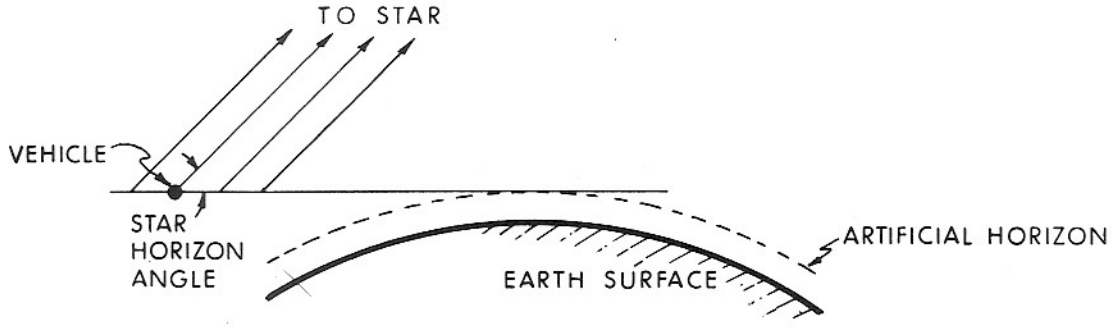

Fig. V-16 Star Horizon Measurement

Since the artificial horizon is at an altitude of approximately 30 kilometers, the angle between the local horizontal and the line to the horizon is about 0.2 radians.

Again it is possible to make a flat earth approximation for this measurement. Figure V-17 illustrates the star horizon measurement when there is no error in the vehicle position. The angle, γ, is the angle between the assumed orbital plane, and a plane containing the vehicle, earth center, and a vector from the vehicle to the star. Thus, when γ is zero, the measurement is insensitive to ϕ errors: when γ is 90°, the measurement is insensitive to θ errors. The angle, $90^{\circ} - \alpha$ is the angle between the velocity vector at time, T_1, and the normal to the plane established by this measurement.

If the measurement is taken at a time, t, when the star horizon angle is equal to the expected star horizon angle at time, T_1, the vehicle is located on a plane (taking the position of the vehicle at time, T_1, as the origin) given by Eq. V-28. One equation relating the errors

$$r(t)\cos\alpha + \gamma(t)\sin\alpha\cos\gamma + \phi(t)\sin\alpha\sin\gamma = 0 \qquad \text{(V-28)}$$

at time, T_1, can be obtained by substitution of Eq. V-13a, b, and c into Eq. V-28. Thus, only one equation between the orbital parameter errors can be obtained from this type of measurement since the measurement involves only one angle and time.

The angle, α, depends only on the orbital altitude. The angle, γ, depends on star direction. It can be chosen to favor either the range error (by making γ small) or the track error (by choosing γ close to 90°). The star horizon angle only determines the time, T_1, when the vehicle should pass through the plane given by Eq. V-28.

Since each measurement provides only one equation in the six unknown orbital errors, it is necessary to take at least six star horizon measurements to determine the orbital parameters.

STAR OCCULTATION MEASUREMENT

As a vehicle moves in an orbit around the earth or moon, stars will rise and set. Whenever a star sets, the disk of the moon or earth occults this star and the vehicle is at that moment crossing a cylinder with its axis in the direction of the

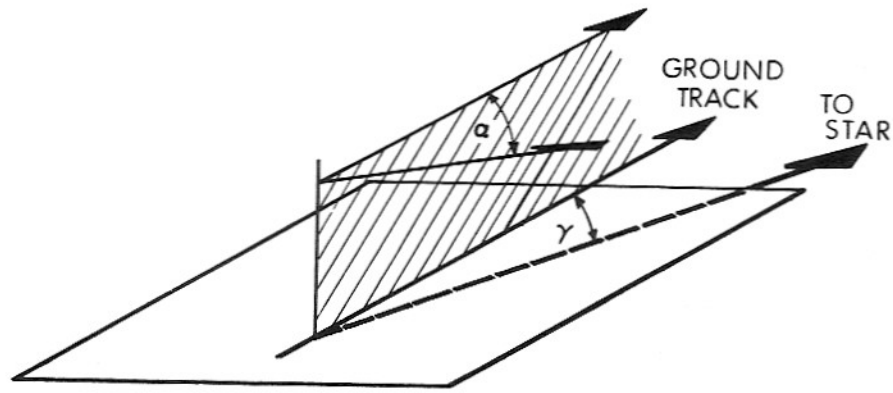

Fig. V-17 Star Horizon Measurement Geometry

star. The diameter of this cylinder is equal to the diameter of the earth or moon.

The measurement is very useful when the vehicle is in a lunar orbit. However, in earth orbit - due to the atmosphere - it is very difficult to determine when a star is occulted since attenuation of the starlight in the atmosphere will take place due to differential refraction, and due to attenuation.

This measurement can be considered as a special case of the star horizon measurement with a zero star horizon angle.

The position of the vehicle is given by the plane defined by Eq. V-28 and the error at time, T_1, by substitution of Eq. 13a, b, and c into Eq. V-28.

Again, six star occultation measurements have to be performed to completely determine the orbital parameters of the vehicle.

The measurements described in this chapter require different configurations of equipment. They also have certain constraints imposed on their usage as described below:

Known Landmark Bearing Measurement:

Advantages: Good error sensitivity
Moderate equipment accuracy requirement with man made beacons usable on both the light and dark side of the earth

Disadvantages: Landmarks have to be chosen for ease of recognition and unambiguity. Cloud cover can make landmarks not useable. Large map requirements. Surveying of some landmarks required. Barely usable on the moon due to poor maps. Requires a reference (e.g. inertial system)

Unknown Landmark Bearing Measurement:

Advantages: Reasonable error sensitivity. Usable anywhere on sunlit side and where ever there are lights on dark side of earth. No maps required. Usable even on the back side of the moon.

Disadvantages: Relatively high equipment accuracy required. Requires a reference (e.g. inertial system)

Star Horizon Measurement:

Advantages: Reasonable error sensitivity
No reference required

Disadvantages: High equipment accuracy required useable only against sunlit earth or moon, requires automatic star tracker and photometer

Star Occultation Measurement:

Advantages: Good error sensitivity
No equipment required

Disadvantages: Usable on moon only.

CHAPTER V-2

MIDCOURSE NAVIGATION

After injection into translunar or transearth orbit, it is no longer possible to use the simplifying assumptions of Eq. V-4 and V-5. Thus, one generally has to resort to computer solutions to solve the navigational problem. Navigation from ground based stations is again possible and has been used quite successful. However, in this part only on-board measurements will be considered.

POSSIBLE MEASUREMENTS

Again in midcourse, as in the orbital case, use is made of optical measurements. However, the accuracy requirements in midcourse are so much greater than the accuracy requirements in orbit that bearing measurements with the inertial system used as a reference are no longer possible. As can be seen from Fig. V-4 and V-5 a measurement uncertainty of one milliradian produces position uncertainties of .15 to .2 km in earth orbit. A measurement with similar accuracy, however, is not too useful at a distance of 100,000 km.

At distances from the earth, which are comparable to the lunar distance, it is possible to use features on the earth or on the moon, or to use planets within our celestial system. Among these choices, the earth and moon provide the best accuracy because of their proximity to the trajectory.

Another factor is of great importance in midcourse. The bearing angles to landmarks or to the horizon change very slowly. In orbit these rates are (see again Fig. V-4 or V-7) in the order of degrees/second. In midcourse the rates reach low values of arc seconds per second. Thus, considerably more time can be taken by the operator to complete each measurement.

Measurements which have been considered are:

Star Landmark Angle Measurements

Star Horizon Angle Measurements
Star Occultation Measurements

The first two of these measurements are sextant measurements. Only one angle has to be read with great accuracy to complete the navigational measurement. The third measurement does not require any instrumentation when a star is occulted by the lunar disc. However, occultation measurements against the earth's disc require relatively precise knowledge of starlight attenuation through the atmosphere to determine a point of occultation. A photometer to make this measurement has not been included in the optical unit.

STAR LANDMARK MEASUREMENT

One precision angular measurement between a star and a landmark places a vehicle on a cone as shown in Fig. V-18. The apex of the cone is located at the landmark. The direction of the center line of the cone is parallel to the direction to the star. The cone half angle is equal to the measured star landmark angle.

Consider the plane formed by the vector from the vehicle to the landmark and the vehicle to the star. If another navigational measurement is made using the same landmark, but another star within this plane, then another cone of position is established as shown in Fig. V-19. The two conical surfaces touch at the line containing the vehicle and landmark. Locally, in the vicinity of the vehicle (assuming a distance to the landmark greater than 20,000 km and a star landmark angle greater than five degrees) this conical surface can be approximated by a plane; the only difference is that for a larger star landmark angle the flat plane approximation is better. No other information is provided by this measurement.

Thus, to obtain information for a second degree of freedom it is necessary to choose another star so that the plane containing the vectors from the vehicle to the second star and vehicle to the first star is approximately orthogonal to the plane shown in Fig. V-18.

The resultant locus of position of the vehicle is a line as shown in Fig. V-20. Any other measurement using the chosen landmark only provides redundant information.

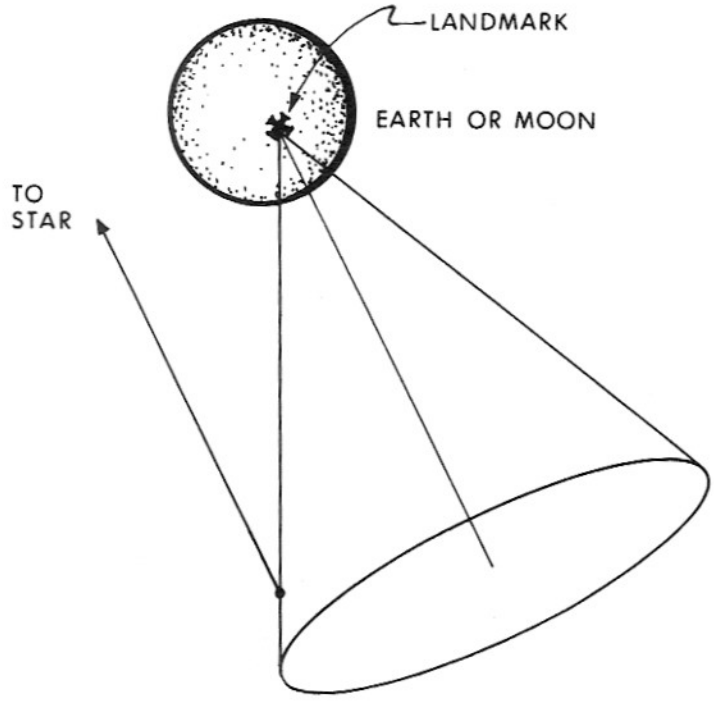

Fig. V-18 Star Landmark Measurement Geometry

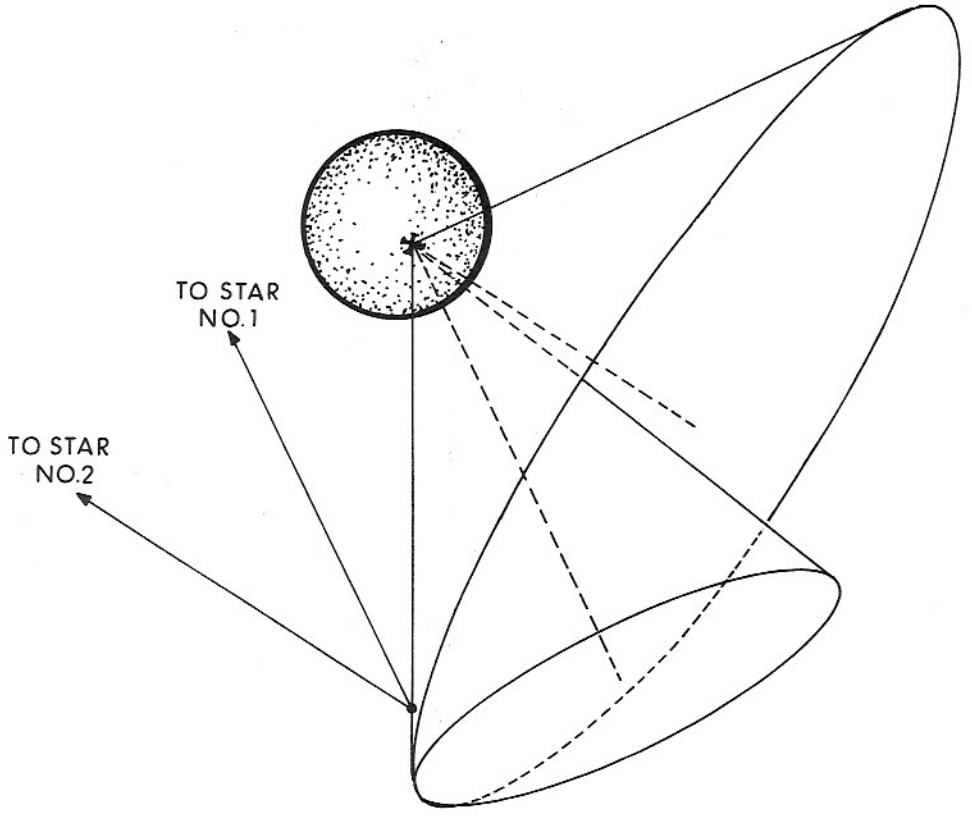

Figure V-19

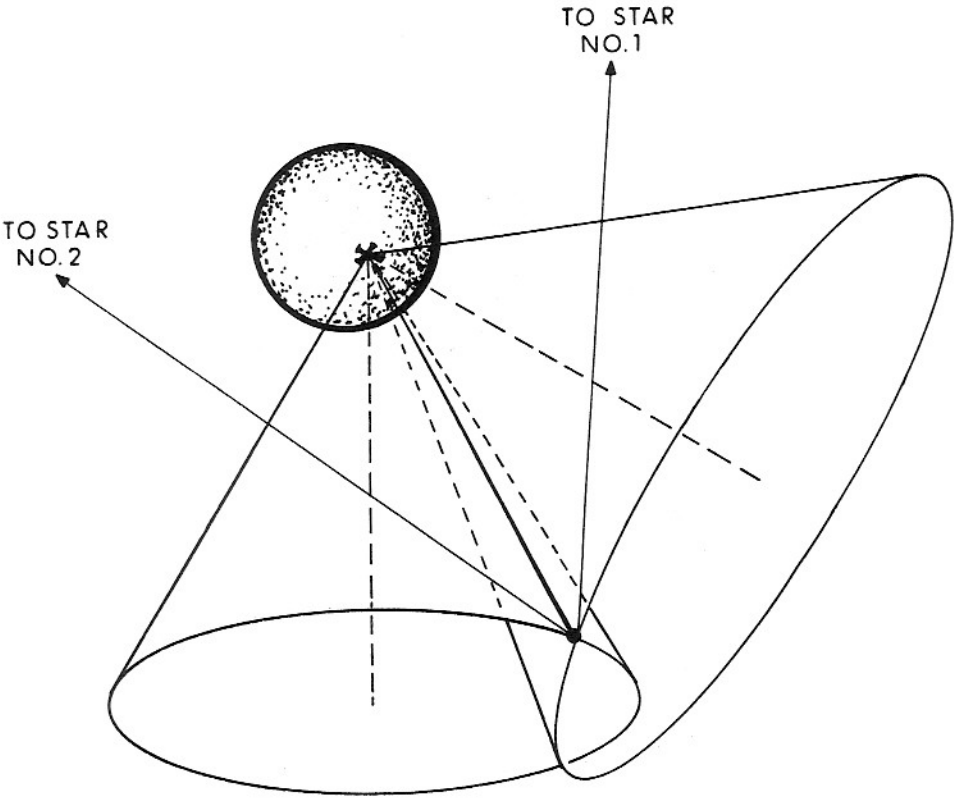

Fig. V-20 Measurement Geometry Using One Landmark and Two Stars

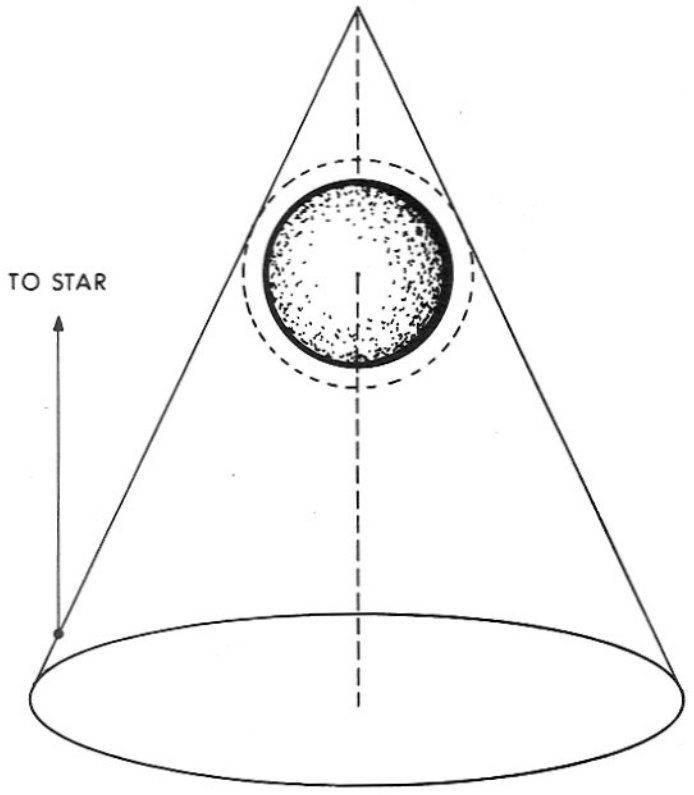

Fig. V-21 Star Horizon Measurement Geometry

The uncertainty of the vehicle along this line can only be reduced if another landmark is used.

Let us assume that a landmark can be used as long as the angle between the line-of-sight and the local vertical at the landmark is less than 45^{o}, then at a 20,000 km distance from the earth, the error along the line established in Fig. V-20 is about .4 km per arc second of error in the measurement. At 100,000 km from the earth star landmark measurements to two earth landmarks provide essentially no additional information when compared to measurements made with only one landmark.

Conversely, it can be said that the choice of earth (or moon) landmarks does not matter for star landmark measurement in midcourse. Any landmark, as long as its position is known and clouds are not present, can be used as well as any other landmark.

STAR HORIZON MEASUREMENT

Let us assume again that a suitable earth horizon as seen from space can be defined. The lunar horizon can be defined by the lunar disc. The astronaut maneuvers the vehicle so that the horizon scan takes place in a plane normal to the horizon. When the measurement between star and horizon is made, the vehicle is located on a cone as shown in Fig. V-21. The center line of the cone is parallel to the starlight. The half angle of the cone is equal to the star horizon measurement angle. The location of the apex of the cone can be obtained from Fig. V-22, where R is the radius of the earth or moon respectively.

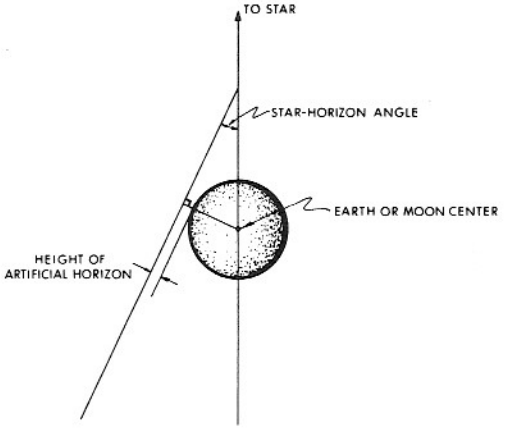

Fig. V-22 Star Horizon Cone Apex Location

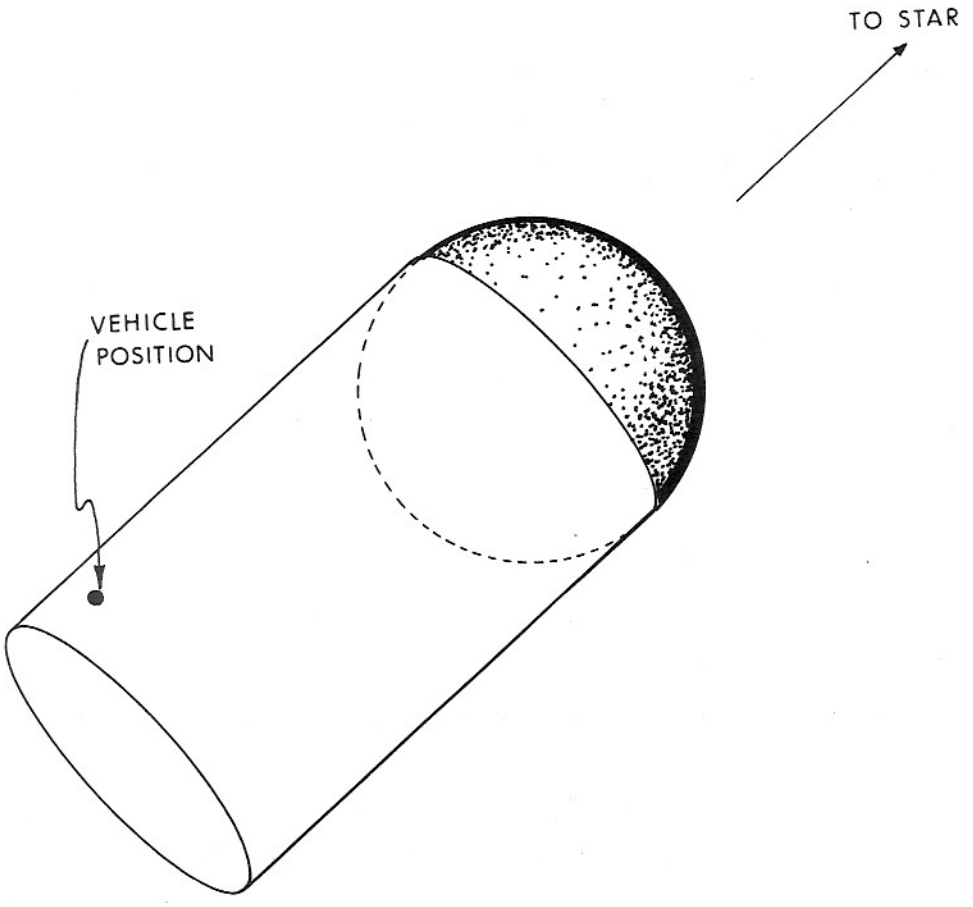

Fig. V-23 Star Occultation Measurement Geometry

Thus, as can be seen, the geometry of a star horizon measurement and a star landmark measurement is almost identical. The only difference between the two measurements is the location of the apex of the cone which defines the vehicle position.

STAR OCCULTATION MEASUREMENT

When a star is occulted by the earth's or moon's disc, the vehicle is located on a cylinder as shown in Fig. V-23. The center of the cylinder passes through the center of the earth. The diameter of the cylinder is equal to the earth's or moon's disc.

Since star occultations depend on the trajectory of the vehicle, it is not possible to choose the measurement geometry to any extent. However, the measurement does have the advantage that no equipment is required to perform it. The only requirement is timing of the star occultation.

ERROR SENSITIVITIES NEAR THE EARTH AND MOON

When the distance between the earth or moon and the vehicle is less than about 20,000 km, the angle between the two horizons is sufficiently large so that an advantage can be gained from star horizon measurements using first one horizon and then the other horizon. Since errors at injection are costliest (from a correction fuel requirement standpoint) when they are made in the plane of the trajectory, it is important to determine their magnitudes early during the midcourse phase.

Let us assume that at the end of injection the venicle has an error in the magnitude of the velocity vector. The direction of the velocity vector and position of the vehicle are assumed to be correct. Figure V-24 shows in exaggerated fashion how the path of the venicle deviates from the nominal (or expected) path. The differences between the actual angles and expected angles are shown in Figs. V-25 to V-29. Let us assume that the vehicle injected with an altitude error of one km. The difference between the expected and actual star horizon angle as defined in Fig. V-24 is shown in Fig. V-25. The error sensitivity for readings taken against either horizon is almost identical when the vehicle reaches a distance of about 30,000 km from earth center (100 minutes after injection). Similar conclusions can be reached from Fig. V-26 (error sensitivity due to wrong injection velocity) and Fig. V-27 (error sensitivity due to an error in the direction of the velocity vector at burnout).

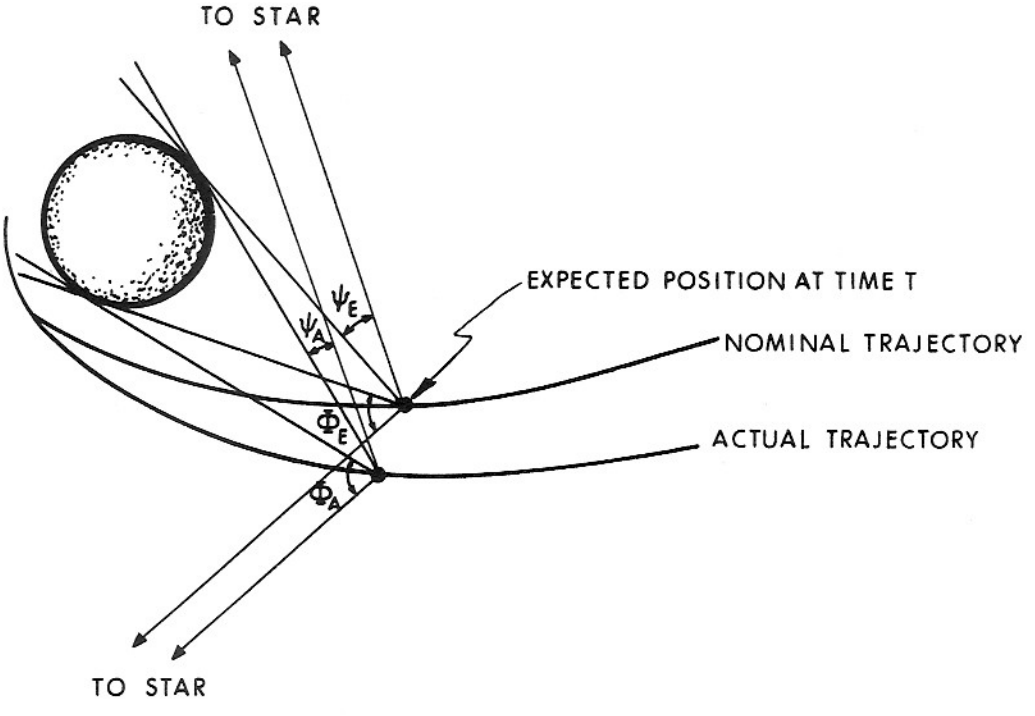

Fig. V-24 Measurements to Both Horizons

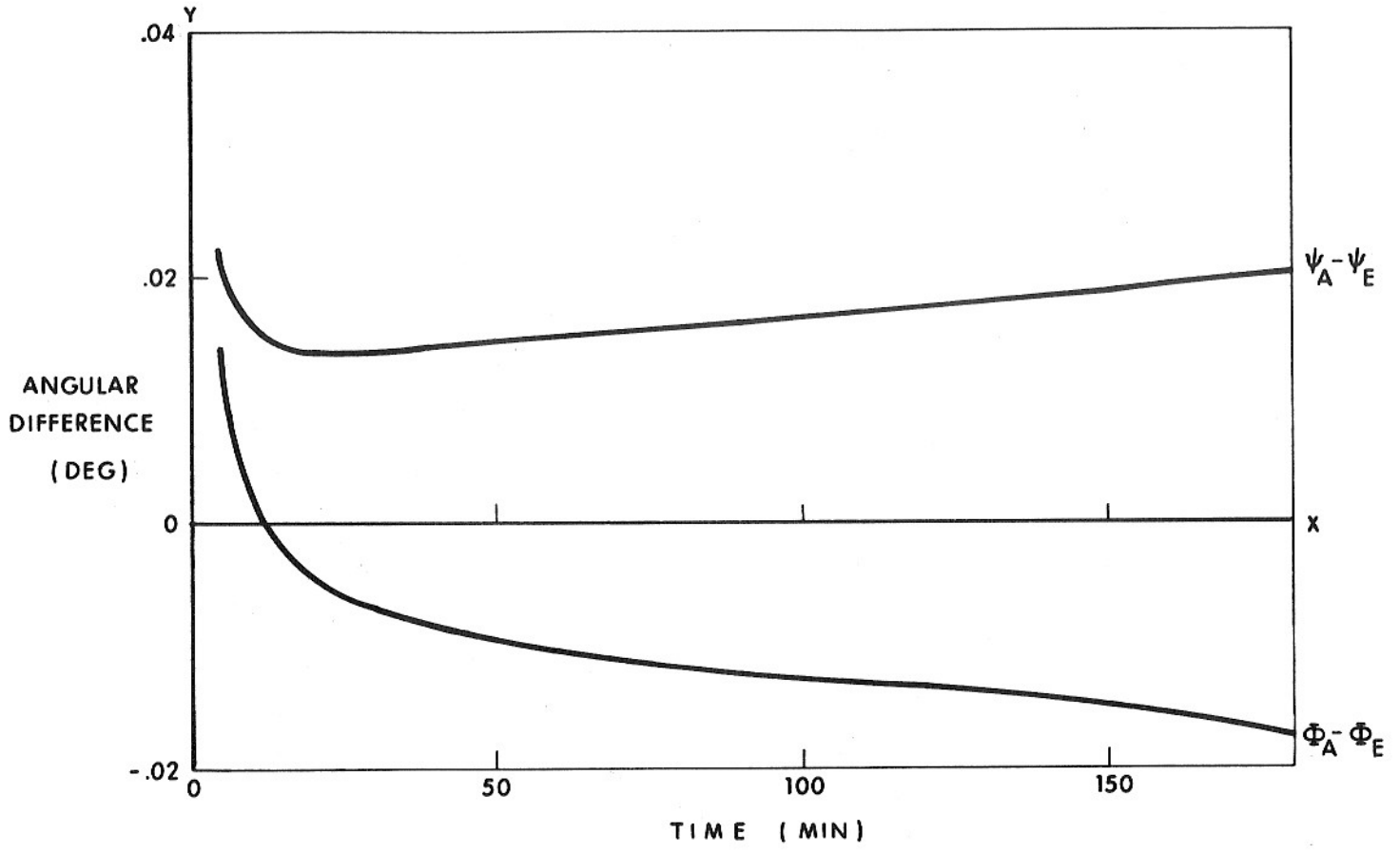

Fig. V-25 Change in Angle Measurement due to Initial Altitude Error

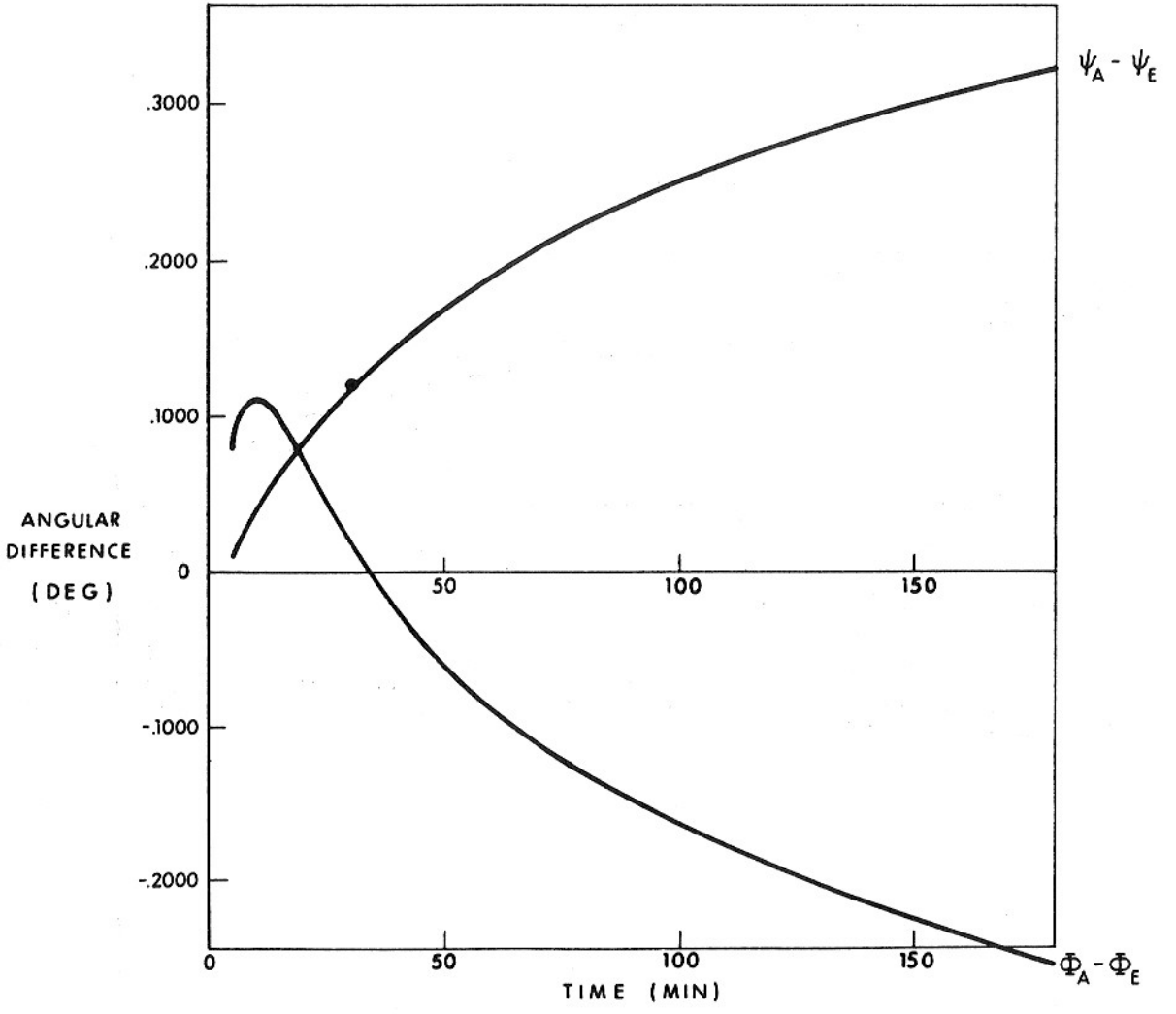

Fig. V-26 Change in Angle Measurement due to Initial Velocity Error of 1 Km/H2

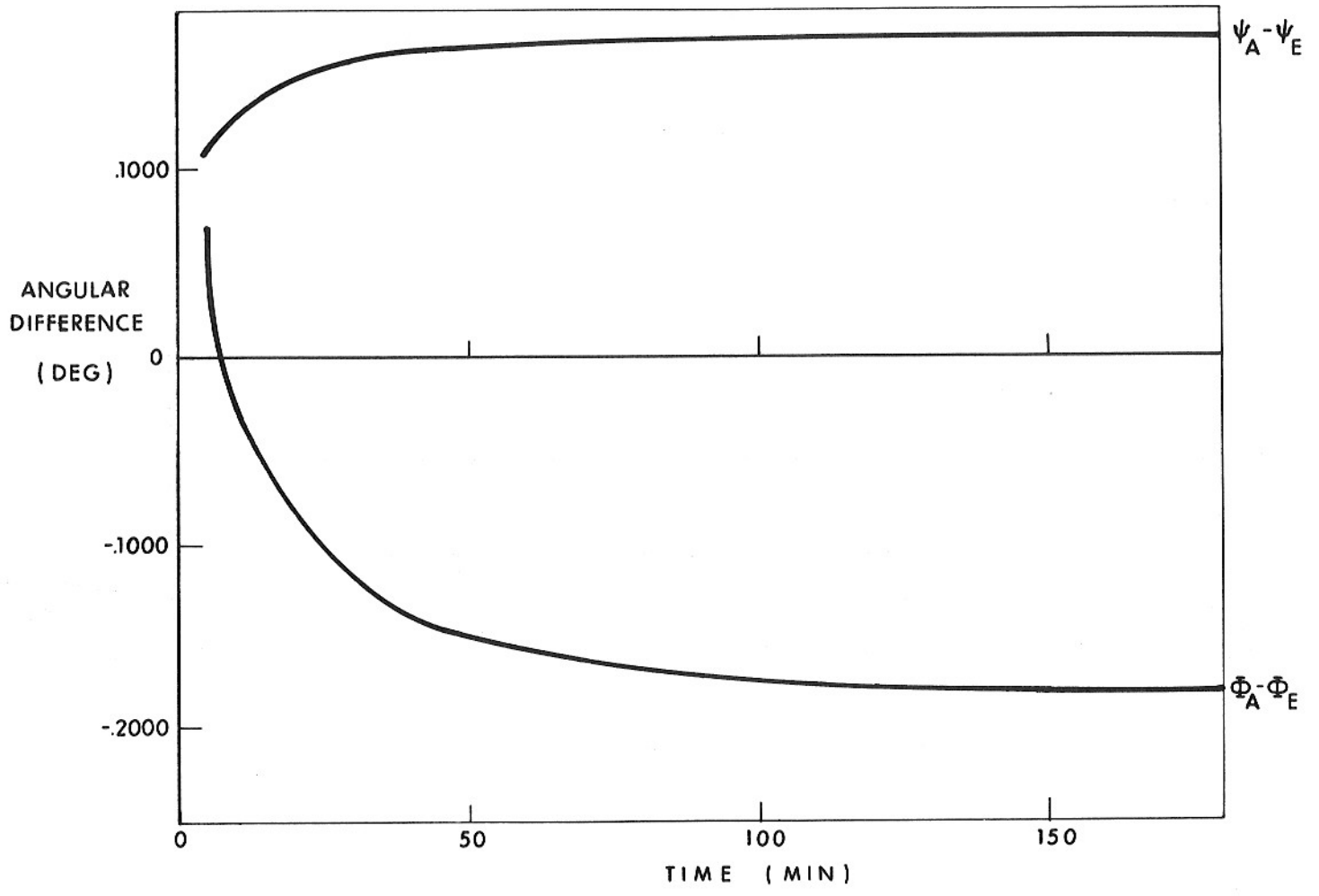

Fig. V-27 Change in Angle Measurement due to Initial Velocity Direction Error of 1 Milliradian

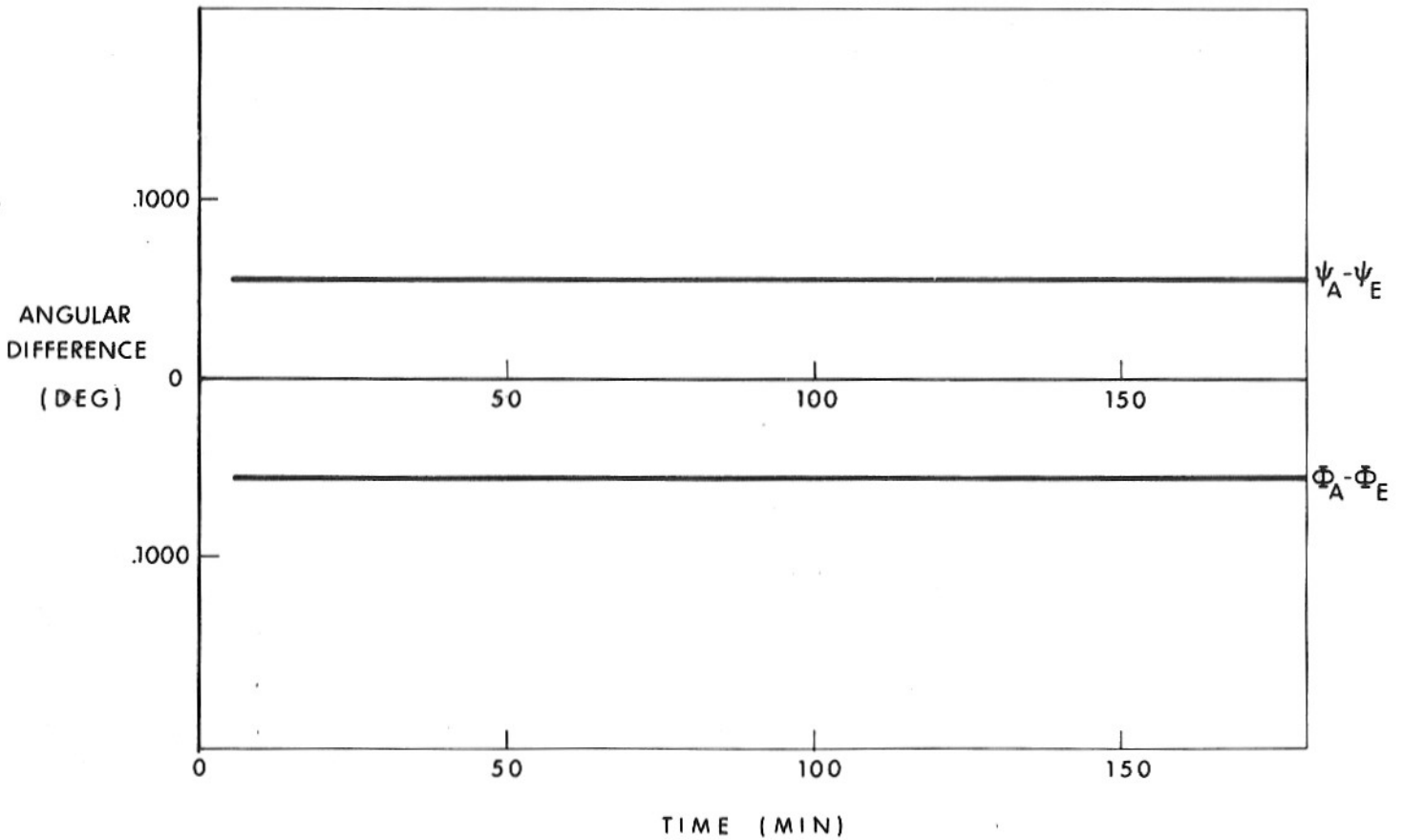

Fig V-28 Change in Angle Measurement due to Initial Range Error of 1 Milliradian

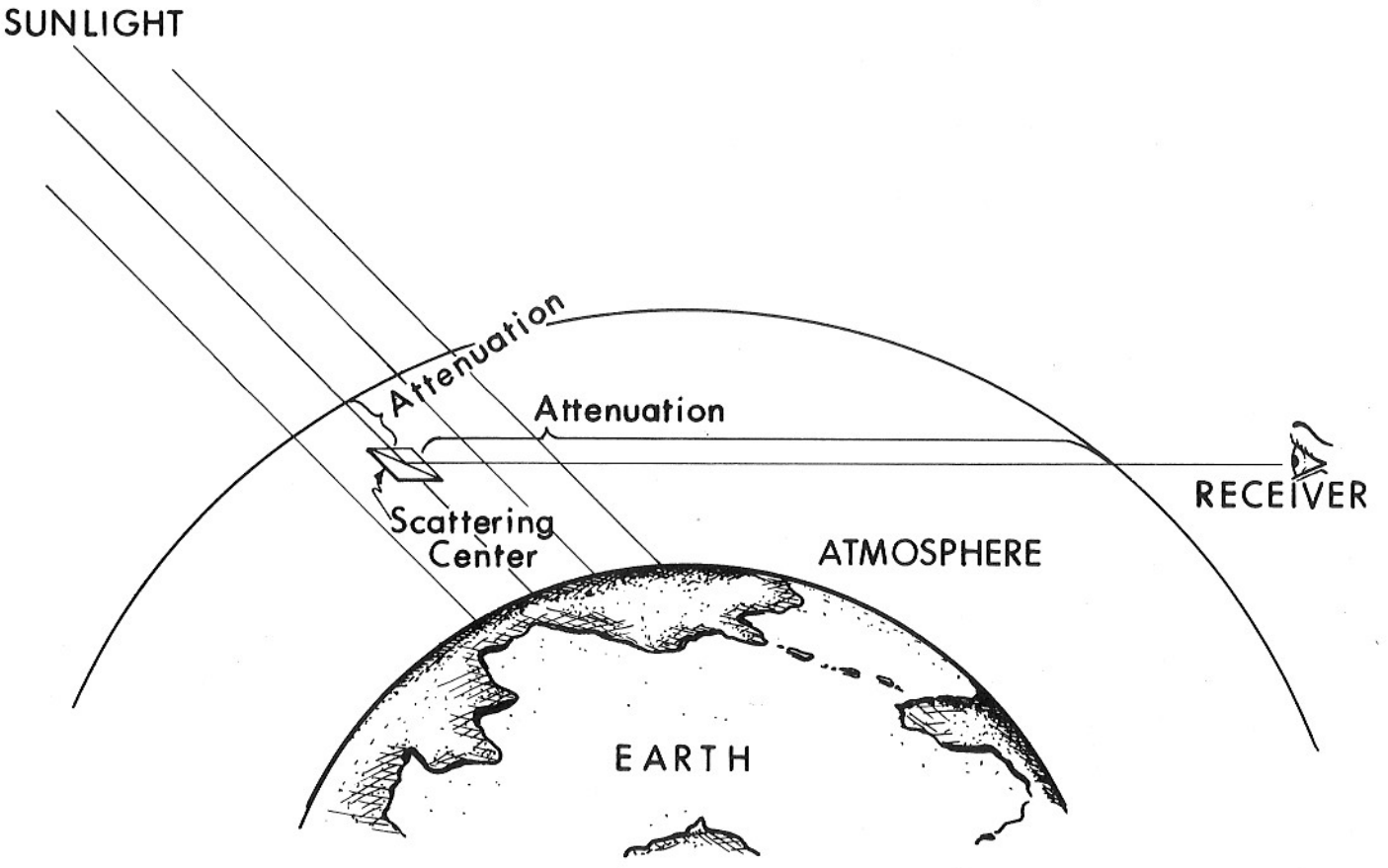

Fig. V-29 Location of Horizon Phenomena

A range error (θ in Chapter I) simply rotates the transfer ellipse by the angular range error θ. Thus, the error sensitivity is constant during the first part of the mission.

If navigational sightings cannot be taken during the first one or one-half hours, either due to crew tasks or constraints imposed by radiation belts, the astronaut or computer has to chose only between an earth feature or a lunar feature. Choosing between specific landmarks or horizon on either the earth or the moon does not provide any major improvement in the knowledge of the vehicle position.

AN ARTIFICIAL EARTH HORIZON

Clouds and atmosphere on the earth, makes it generally impossible to see the earth's surface near the horizon; thus it is necessary to define a horizon which is sufficiently high above the clouds to be visible during most of the mission time.

To date, most of the horizon sensing has been accomplished in the infrared region of the spectrum. However, sunlight scattered within the earth's atmosphere also provides a possible horizon. Since the upper atmosphere scatters most of the blue and near ultraviolet light, a horizon model based on scattered sunlight is being used. Figure V-29 illustrates the measurement geometry used. A comparison is made between the maximum intensity and 1/2 of the maximum. The 1/2 max. establishes a horizon located about 30 km above the earth's surface.

CHAPTER V-3

THE APOLLO OPTICAL UNIT

The varied navigational measurements which are made during the Apollo mission are used as a basis for the design of the optical unit shown in Fig. V-30 The unit consists of a sextant, an automatic star tracker and photometer, and a scanning telescope.

During midcourse when it is necessary to make accurate star landmark and star horizon measurements, the sextant is used. The scanning telescope is used only as an instrument for target acquisition.

Both instruments are used during the midcourse portion of the mission. The scanning telescope is used for known landmark bearing measurements. Its large field of view is essential for landmark identification and acquisition. The movable line-of-sight of the sextant is used for unknown landmark tracking. The automatic features are used for star-horizon measurements. Star occultation measurements need no particular bearing read out since only the time of occultation is required. Either instrument or a window can be used for this particular measurement.

SPACE SEXTANT

The sextant consists of a 28 power, 1.8 degree field of view telescope located within the optical base (see Fig. V-30). Before light enters the telescope, it passes through the sextant head, where the two lines-of-sight of the instrument are combined.

The landmark line-of-sight passes through the beamsplitter and from there directly into the telescope. To move this line-of-sight, it is necessary to move the vehicle. The beamsplitter passes about 20 percent of the light to the telescope. Also contained within the beamsplitter is a filter, which attenuates most of the blue and green light entering the landmark line-of-sight. This reduces the blue haze which is generally visible on the earth from high altitudes without appreciably degrading the characteristics of lunar landmarks.

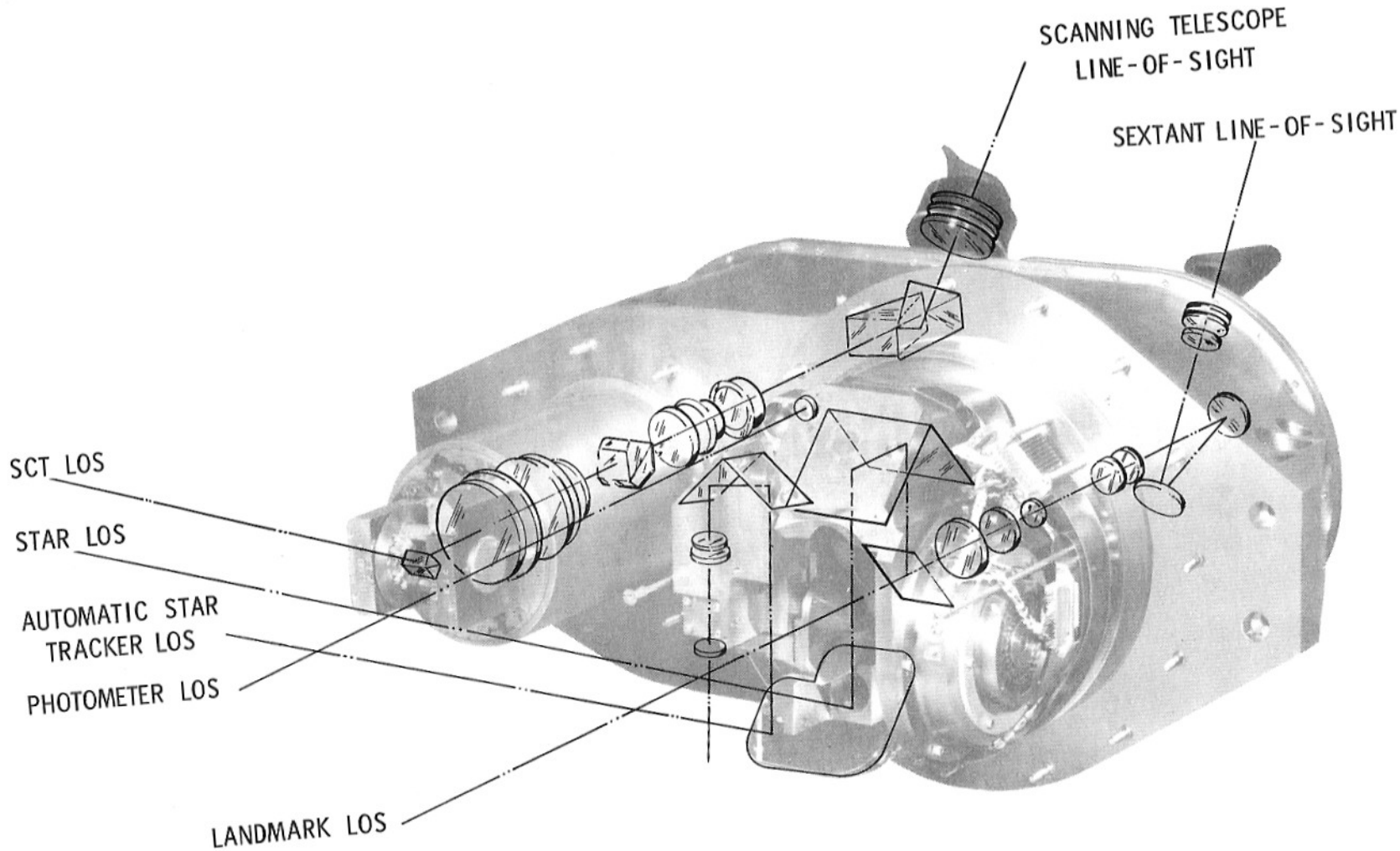

V-30 Apollo Optical Unit

The star line-of-sight is directed to the telescope by a movable mirror, two fixed mirrors, and the beamsplitter. About 80 percent of the starlight passes through the beamsplitter into the telescope.

The movable mirror is positioned by a conventional A.C. servo system. The read out of the mirror position (this is the most accurate angle read out within the guidance system) depends on a 64 speed (128 pole) resolver. The angles of this resolver are read by a coupling data unit as described in Part IV.

Angles ranging from zero to 50 degrees between the two lines-of-sight can be read with this instrument. The mirror can be moved further to 90 degrees, where the image of the reticle is reflected back upon itself. The astronaut can use this point as a check of the alignment stability of the instrument. Viewing of a bright star or planet with the line-of-sight angle set to zero degrees provides another point where the sextant angular read out can be easily checked. These self-checking features have been incorporated to make sure that a check of the instrument accuracy can be made before and after each midcourse navigational sighting.

The head assembly and telescope rotate within the optical base. This motion provides the second degree of freedom of motion for the star line-of-sight. Motion in this direction is limited to $\pm$ 270 degrees from a predetermined zero. The power to the components located on the sextant head is carried through a flex cable. Limitation of the freedom of motion of the sextant thus makes use of slip rings not required.

STAR TRACKER-PHOTOMETER

The star tracker is included within the optical unit to enable the astronaut to make measurements between the earth's horizon and a star. Both instruments including their detectors and preamplifiers are completely located on the sextant head.

The photometer measures the intensity of the near ultraviolet sunlight scattered by the earth's atmosphere. Light collected by the photometer aperture is filtered and modulated by a vibrating reed before it reaches the photodetector. The signal is further amplified and the level of the signal is detected with circuitry within the power and servo assembly of the guidance system.

The star tracker is a narrow, field-of-view (1/2 deg. X 1/2 deg.) instrument.

Star light is directed into the aperture of the telescope by the star line-of-sight movable mirror and two redirection mirrors. Crossed tuning forks are used to provide information about the star position within the tracker' s field of view. The electronics required to process the star tracker signal are also located in the power and servo assembly.

The two degrees of freedom required to position the star tracker are identical to the degrees of freedom provided for the star line-of-sight. Thus, when a star is tracked the astronaut can compare the star position in the sextant field to the center of the reticle. This provides a visual check on the operation of the star tracker.

SCANNING TELESCOPE

The scanning telescope is a single line-of-sight, unit power, 60 degree field of view instrument used for making known landmark bearing measurements in earth and lunar orbit and also for general use, such as acquisition of landmarks and stars for sextant sightings.

The complete telescope assembly rotates within the optical base, similar to the sextant. The two shafts are continuously tied together with a conventional A. C. servo system.

The light enters the telescope through a double dove prism. This prism can be positioned so that the telescope line-of-sight is parallel to the landmark line-of-sight (for midcourse landmark acquisition) or parallel to the star line-of-sight for star acquisition. A third position, offset from the landmark line-of-sight by 25 degrees, is also provided. In this position the scanning telescope covers the complete sextant field of view. This position is used when the astronaut tries to hold one image in one of the sextant lines-of-sight while searching for the second image.

To provide backup in case of an electrical failure, the scanning telescope also contains two mechanical counters connected to the movable parts of the telescope. These counters can be read and the angles manually entered into the computer in case of a malfunction within the angle encoding loop.

Two knobs which can be used for manual positioning of the telescope line-of-sight are also provided. These provide a backup for the A. C. servo components which are normally used to position the sextant and scanning telescope.

BIBLIOGRAPHY

Chandrasekhar, S., Radiactive Transfer, Dover Publications 1960

Peterson, R., Final Report on Special Techniques for Space Navigation, Control Data Corporation, July 1964

Seward, H.H., The Blue-White Boundary Horizon Sensor, MIT Instrumentation Laboratory Report E-1206, September 1962

Wolff, M., The Profile of an Exponential Atmosphere Viewed from Outer Space and Consequences for Space Navigation, MIT Instrumentation Laboratory Report E-1634, September 1964

Zucherbraun, J.,"High-Reliability Scanners for Stellar Navigation", Electronics, May 11, 1962